Activation of the STAT1 Pathway Accelerates Periodontitis in *Nos3*$^{-/-}$ Mice

W. Wei, X. Xiao, J. Li, H. Ding, W. Pan, S. Deng, W. Yin, L. Xue, Q. Lu, Y. Yue, Y. Tian, M. Wang, and L. Hao

Appendix

Materials and methods

Micro-computed tomography (micro-CT) scanning and analysis. Micro-CT scanning of maxillae was performed on a vivaCT80 system (SCANCO Medical; Zurich Switzerland). The alveolar bone was defined as the region of interest (ROI) with a spatial resolution of 7 μm(Park et al. 2007). According to the ROI, bone volume/total volume (BV/TV), trabecular number (Tb.N), and trabecular separation (Tb.Sp) were calculated for quantification. As described previously (Sasaki et al. 2008), we captured all images of these maxilla samples by 3D reconstruction to analyze the periodontal bone loss. The mesial and distal edges of the exposed tooth root, the alveolar ridge, and the cement-enamel junction were enclosed in a polygonal area, and then examined using Image analysis software. Measurements are expressed in mm^2.

Histological analysis. Decalcified maxilla samples were sectioned using a routine procedure (Li et al. 2019). Hematoxylin and eosin stain (H&E) staining was performed using a commercially available kit (CAT# C0105, Beyotime, China).

Enzyme-linked immunosorbent assay (ELISA). According to the standard protocol, we used commercial ELISA kits to detect cytokines in the cell-culture supernatant and *in vivo* serum samples: TNFα (CAT# 88-7324-82, Thermo Fisher Scientific, USA) and IL6 (CAT# 88-7064-86, Thermo Fisher Scientific, USA). Results are expressed as pg/ml.

Quantitative Real-Time PCR. The total RNA of gingival tissue and alveolar bone in the mandible lesion area *in vivo* and *in vitro* samples was extracted using the RNA Extraction Kit (CAT# 9766, Takara Bio, USA). RNA was reverse-transcribed with the Vilo® Master Kit (CAT# 11756050, Invitrogen, USA) amplified using SYBR Mix (CAT# RR430S,

TaKaRa Bio, USA), and detected on an RT-PCR detection system (ABI, USA). Primers were used to amplify the following genes **(Appendix Table 1)**: *Stat1, Cxcl9, Socs3, Stat3, Il10, Tnfα, Il6, Ifnγ, Il1β, F4/80, CD19, CD3, CD11b, AngII, Nos3, Agtrap, Tlr4* and *Gapdh*. Gene expression data were quantified by the ΔΔCt method and presented as a ratio to *Gapdh* expression. These experiments were conducted independently in triplicate.

Immunohistochemistry (IHC) and Immunofluorescence (IF) analysis. Maxilla sections were used for IHC analysis according to the manufacturer's instructions with the following antibodies: rabbit monoclonal pSTAT1 (Cat#9176, Cell Signaling Technology, USA) and pSTAT3 (Cat#9145, Cell Signaling Technology, USA). We performed this analysis using the Vectastain Elite ABC-HRP kit (PK-6100, Vector Laboratories, USA). For IF analysis, the sections and cells were incubated with STAT1 (Cat#14994, Cell Signaling Technology, USA), STAT3 (Cat#9139, Cell Signaling Technology, USA), F4/80 (Cat#30325, Cell Signaling Technology, USA), CD19 (Cat#3574, Cell Signaling Technology, USA), CD11b (Cat#52478, Abcam, USA) and CD3 (Cat#sc-20047, Santa Cuz, USA) primary antibodies, followed by Alexa Fluor 555-conjugated secondary antibodies (Cat#A32727, Cat#A32732, Invitrogen, USA). The sections were then stained with DAPI (Cat#28718-90-3, Sigma Aldrich, USA) to locate the nuclei. The number of pSTAT1, pSTAT3, F4/80, CD3, CD19 positive cells per maxilla area was counted with a microscope, and expressed as a percentage of the total number of cells (Beklen et al. 2008).

Western Blotting. As previously described, we isolated the proteins from the right mandibular lesion region, and separated and transferred to nitrocellulose membranes (Nogueira et al. 2014). The membranes were blocked with 5% BSA for 1 hour and incubated overnight at 4°C with the primary antibodies including pSTAT1, pSTAT3, STAT1, STAT3, IL10, GAPDH (Cat#9176, 9145, 14994, 9139, 12163, 5174, Cell Signaling Technology, USA), and SOCS3 (Cat#16030, Abcam, USA). Subsequently, HRP-conjugated antibodies were applied to the membranes, and the signals were detected using the ChemiDoc-It 600 Imaging System (Fisher Scientific, USA). Finally,

densitometric analysis was performed using an ImageJ analysis system. All experiments were repeated 3 times independently.

Harvesting and preparation of samples. After 56 days of the initial bacterial infection, animals were sacrificed by CO_2 hypoxia. The left maxilla samples were dissected and used for micro-CT analyses, and the right maxilla samples were fixed in 4% formaldehyde and used for histological analyses. The left mandibular bones were used for RNA extraction and the right mandibular for protein extraction to prepare samples for qRT-PCR and western blot assays, respectively. Whole blood from the orbital vein was collected to separate serum for the ELISA.

Cell culture and stimulation. RAW 264.7 (macrophage cell line) were cultured in Dulbecco's modified Eagle's medium (Corning, NY, USA) supplemented with 10% fetal bovine serum (Omega Scientific, USA). L929 (fibroblasts cell line) were cultured in minimum essential medium (Corning, NY, USA) supplemented with 10% fetal bovine serum (Omega Scientific, USA). Raw 264.7 and L929 were plated at 5×10^5 cells/ml in 6-wells plates for mRNA extraction, western blot, and ELISA. Cells were then stimulated with or without 100 nM Ang II (Cat#A9525, Sigma–Aldrich, USA) (Meng et al. 2017) and 200 ng/ml LPS (Cat#L3024, Sigma–Aldrich, USA) (Meng and Lowell 1997) for 12 hours, followed by sample collection. The concentration and stimulation time were determined in a preliminary study.

Bone marrow-derived monocytes culture. After the wild type and *Nos3* knockout mice (8-10 weeks old) were sacrificed, the femurs and tibias were separated and the medullary cavity was flushed with MEM medium. After centrifugation at 500 g for 8 mins, the supernatant was discarded. Resuspend the cells with the MEM medium (supplemented with 10% FBS and 20ng/ml M-CSF) (Francke et al. 2011).

Blood pressure measurement. Blood pressure measurements were applied using the CODA tail-cuff system as described (Daugherty et al. 2009). The systolic and diastolic blood pressure was measured at 16 weeks for each group.

Concentration selection for *in vitro* experiment. At a concentration of 200 ng/ml, LPS had the highest effect on STAT3 phosphorylation and elevated inflammatory factor mRNA levels (**Appendix Figure 8, 9**). AngII had the highest effect on STAT1 phosphorylation at 100 nM (**Appendix Figure 9**). After 12 hours of stimulation, the groups showed significant difference (**Appendix Figure 10**).

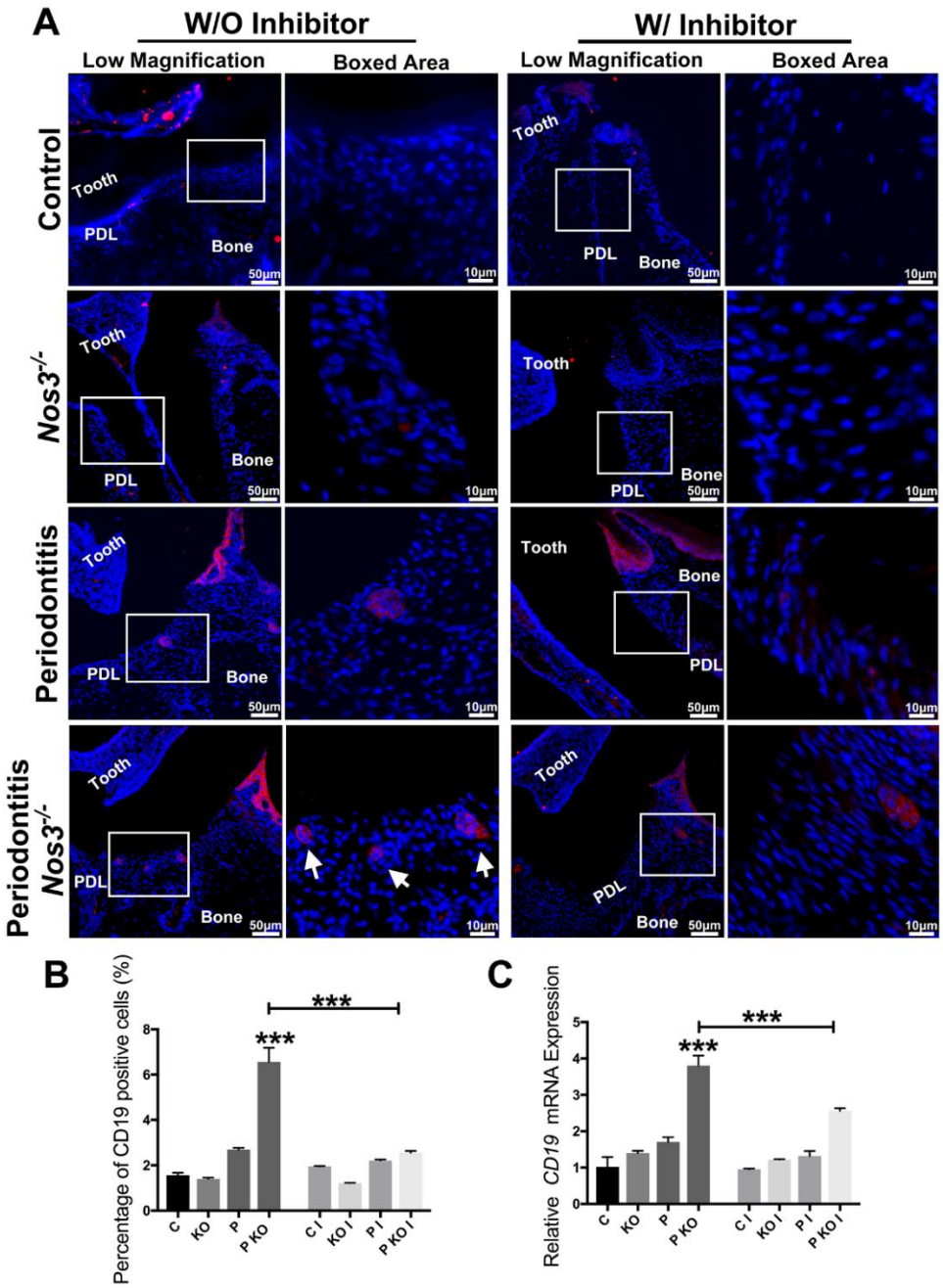

Appendix Figure 1. Effect of STAT1 inhibition on B-lymphocytes infiltration. (A) IF staining of CD19 positive (red) B-lymphocytes in periodontitis lesion area in different groups. The positive stained cells are showed in white inset boxes of enlarged images. **(B)** Quantification of CD19 positive B-lymphocytes numbers in the periodontal area are shown. **(C)** The mRNA expressions of *CD19* in different groups were detected by qRT-PCR. C: non-nephritic phosphate-buffered saline (PBS)-treated group, KO: Nos3 knockout group, P: periodontitis group, P KO: periodontitis with Nos3 knockout group, I: inhibitor treated group. ***: $p<0.001$, repeated 3 times. Data are presented as the mean ± SD (n = 10 per group), compared with the Control.

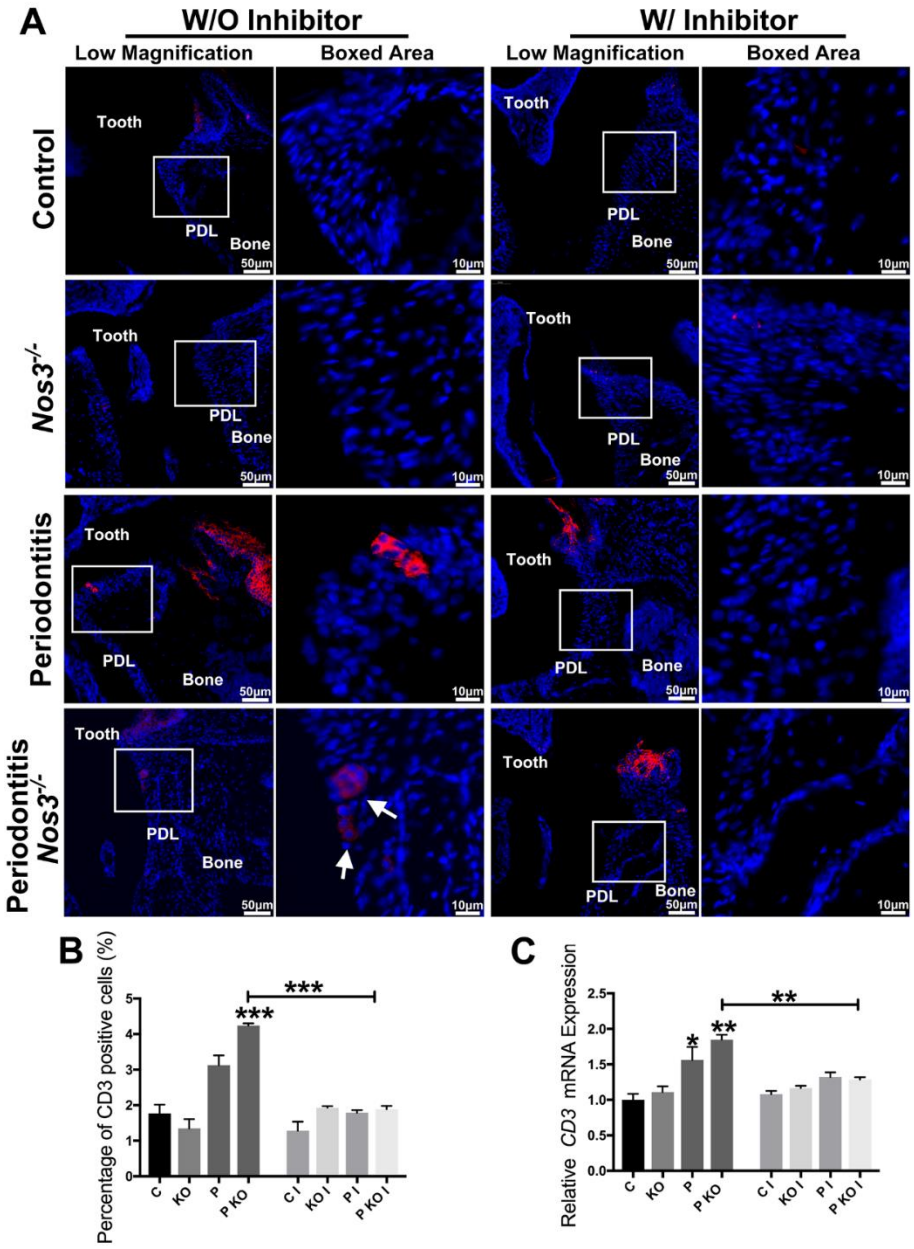

Appendix Figure 2. Effect of STAT1 inhibition on T-lymphocytes infiltration. (A) IF staining of CD3 positive (red) T-lymphocytes in periodontitis lesion area in different groups. The positive stained cells are showed in white inset boxes of enlarged images. **(B)** Quantification of CD3 positive T-lymphocytes numbers in the periodontal area are shown. **(C)** The mRNA expressions of *CD3* in different groups were detected by qRT-PCR. C: non-nephritic phosphate-buffered saline (PBS)-treated group, KO: Nos3 knockout group, P: periodontitis group, P KO: periodontitis with Nos3 knockout group, I: inhibitor treated group. *: $p<0.05$, **: $p<0.01$, ***: $p<0.001$, repeated 3 times. Data are presented as the mean ± SD (n = 10 per group), compared with the Control.

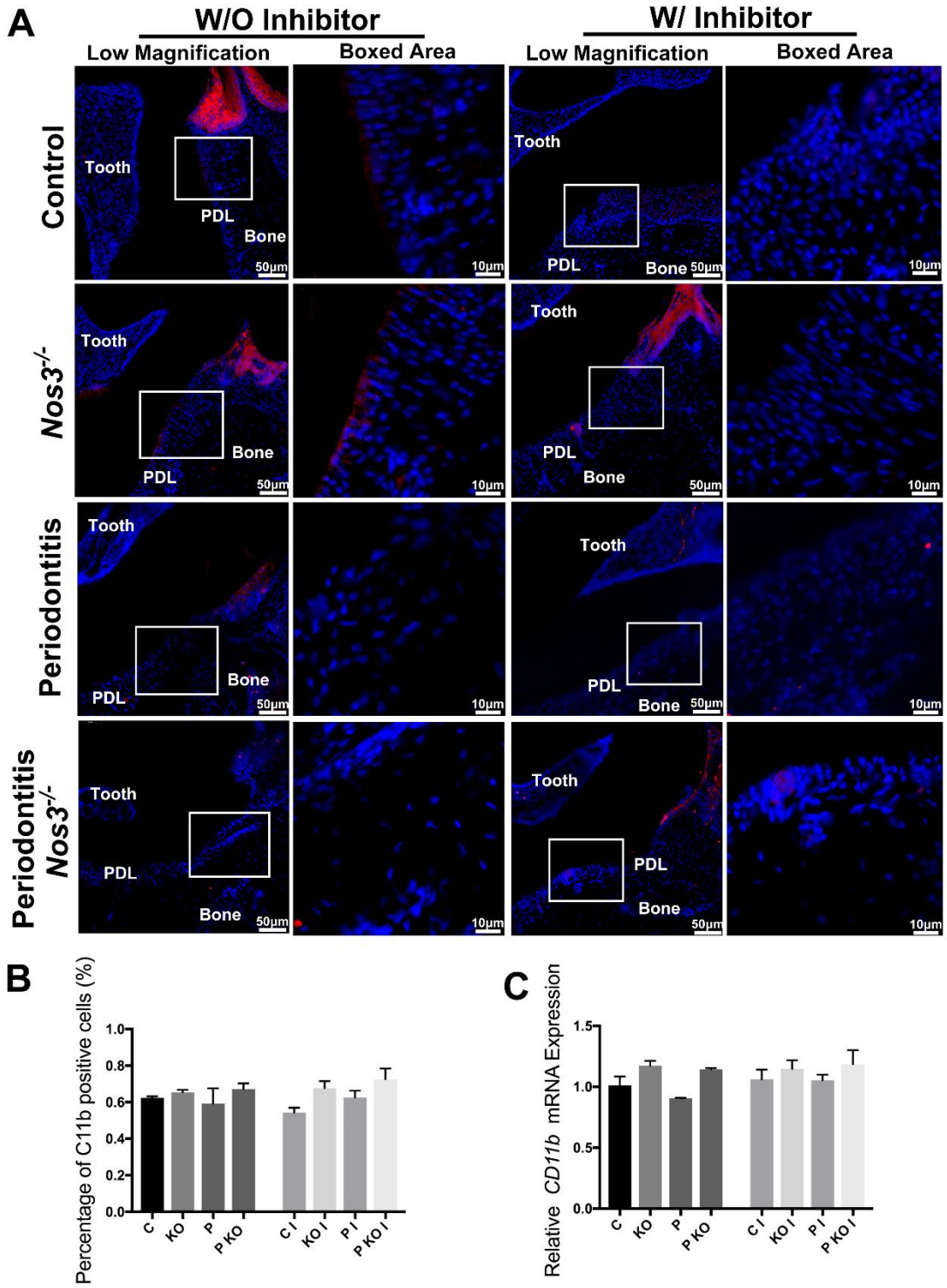

Appendix Figure 3. Effect of STAT1 inhibition on neutrophils infiltration. (A) IF of CD11b positive (red) neutrophils in periodontitis lesion area in different groups. The positive stained cells are showed in white inset boxes of enlarged images. **(B)** Quantification of CD11b positive neutrophils numbers in the periodontal area are shown. **(C)** The mRNA expressions of *CD11b* in different groups were

detected by qRT-PCR. C: non-nephritic phosphate-buffered saline (PBS)-treated group, KO: Nos3 knockout group, P: periodontitis group, P KO: periodontitis with Nos3 knockout group, I: inhibitor treated group. Repeated 3 times. Data are presented as the mean ± SD (n = 10 per group), compared with the Control.

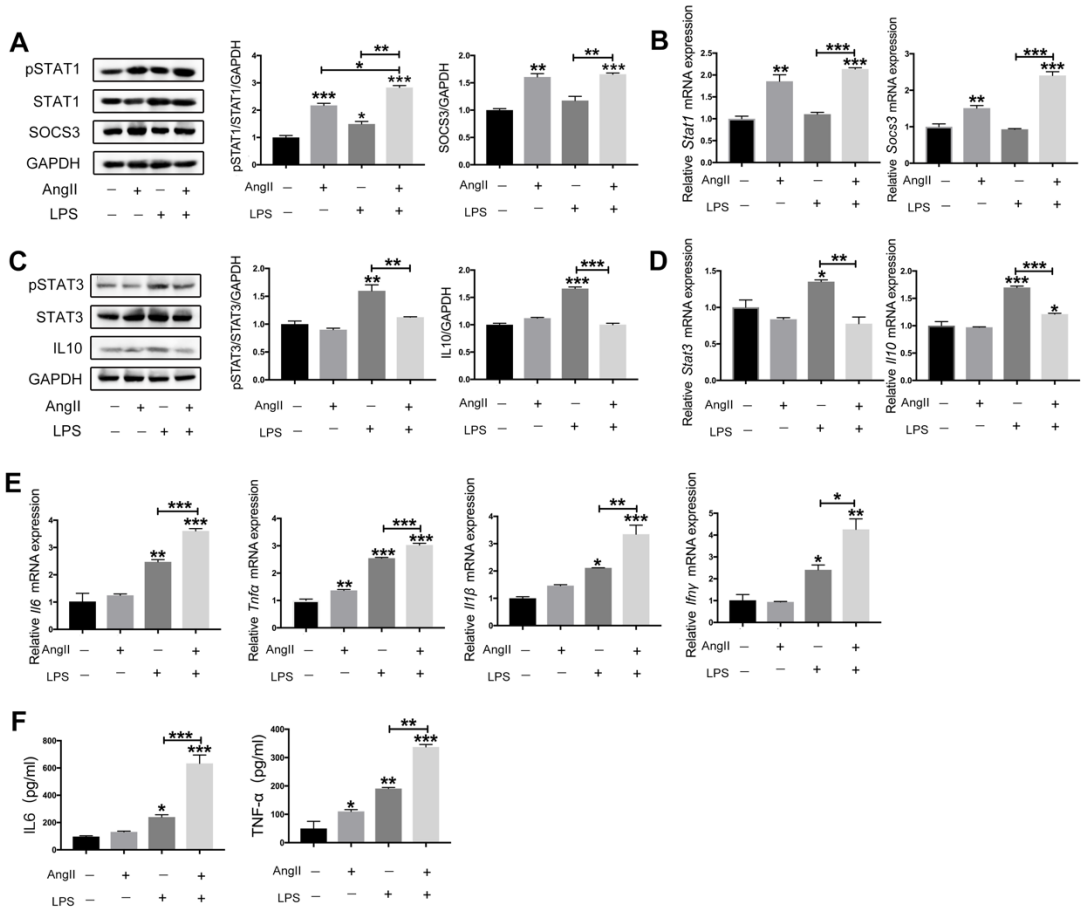

Appendix Figure 4. Effect of Ang II and LPS on STAT1 and STAT3 phosphorylation and related chemokine expression in L929 fibroblasts. (A) Western blot analysis of pSTAT1, STAT1 and SOCS3 expression in different groups, representative images and the summary of the normalized quantification are shown. **(B)** The mRNA expressions of *Stat1* and *Socs3* in different groups were detected by qRT-PCR. **(C)** Western blot analysis of pSTAT3, STAT3 and IL10 expression in different groups, representative images and the summary of the normalized quantification are shown. **(D)** The mRNA expressions of *Stat3* and *Il10* in different groups were detected by qRT-PCR. **(E)** qRT-PCR of pro-inflammatory chemokine in the different groups. **(F)** ELISA analysis of IL6 and TNFα in different groups. Fibroblasts were treated with or without Ang II (100nM) and LPS (200ng/ml) for 12 hours. *: $p<0.05$, **: $p<0.01$, ***: $p<0.001$, repeated 3 times. Data are presented as the mean ± SD, compared with the Control.

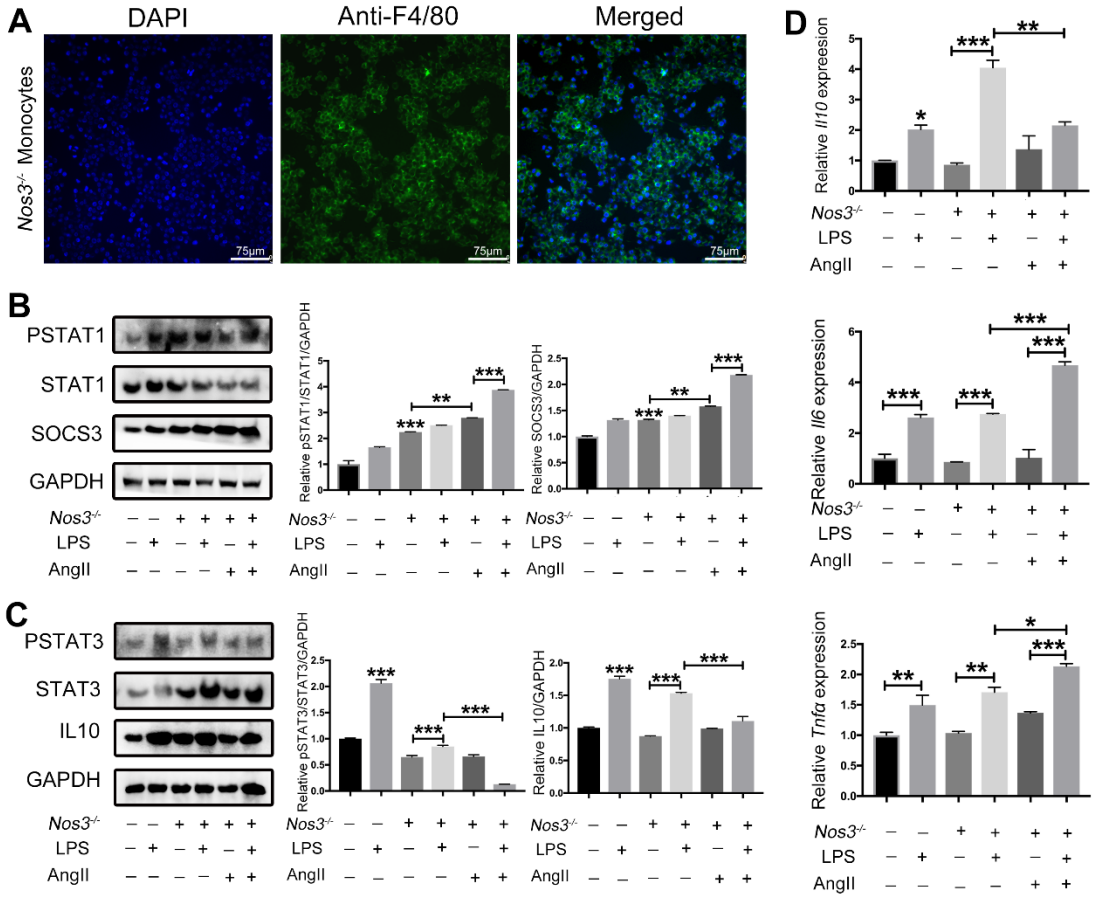

Appendix Figure 5. Effect of LPS and AngII on STAT1 and STAT3 phosphorylation and related chemokine expression in monocytes from *Nos3*$^{-/-}$ mice. (A) IFC of F4/80 positive (green) bone marrow derived monocytes. **(B)** Western blot analysis of pSTAT1, STAT1 and SOCS3 expression in different groups, representative images and the summary of the normalized quantification are shown. **(C)** Western blot analysis of pSTAT3, STAT3 and IL10 expression in different groups, representative images and the summary of the normalized quantification are shown. **(D)** The mRNA expressions of *Il10, Il6* and *Tnfα* in different groups were detected by qRT-PCR. Monocytes were treated with or without Ang II (100nM) and LPS (200ng/ml) for 12 hours. *: p<0.05, **: p<0.01, ***: p<0.001, repeated 3 times. Data are presented as the mean ± SD, compared with the Control.

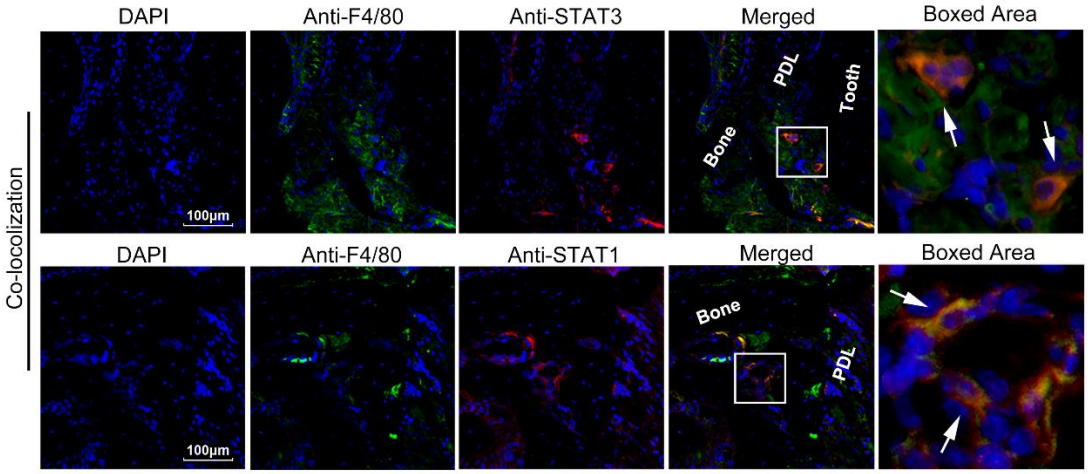

Appendix Figure 6. Co-localization of F4/80 with STAT1 and STAT3 in the periodontitis lesion area. Co-localization of F4/80 (green) with STAT1 (red) or STAT3 (red) in the periodontitis lesion area. White arrow refers to cells that are co-expressed. The results are representative of three independent experiments. PDL: Periodontal ligament.

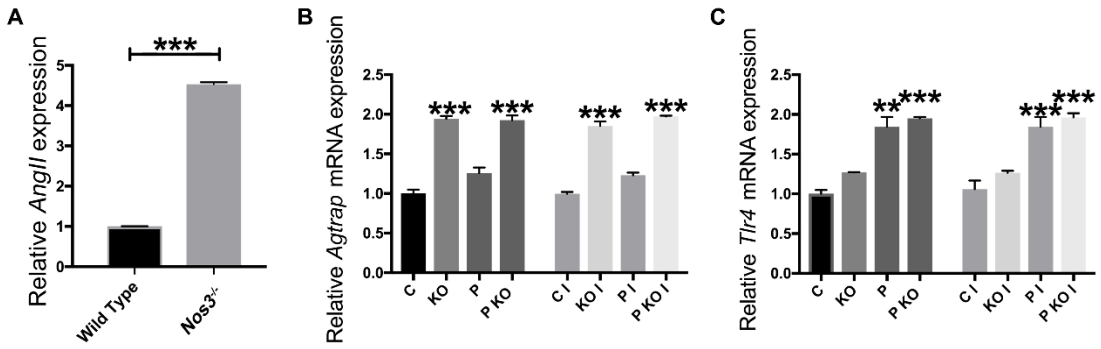

Appendix Figure 7. Expression of AngII, AT1 receptor and TLR4 receptor *in vivo.* Relative mRNA expression levels of *AngII*, *Agtrap* and *Tlr4* were detected by qRT-PCR. *Gapdh* was used as the endogenous control. *: $p<0.05$, **: $p<0.01$, ***: $p<0.001$, repeated 3 times. Data are presented as the mean ± SD (n = 10 per group), compared with the Control.

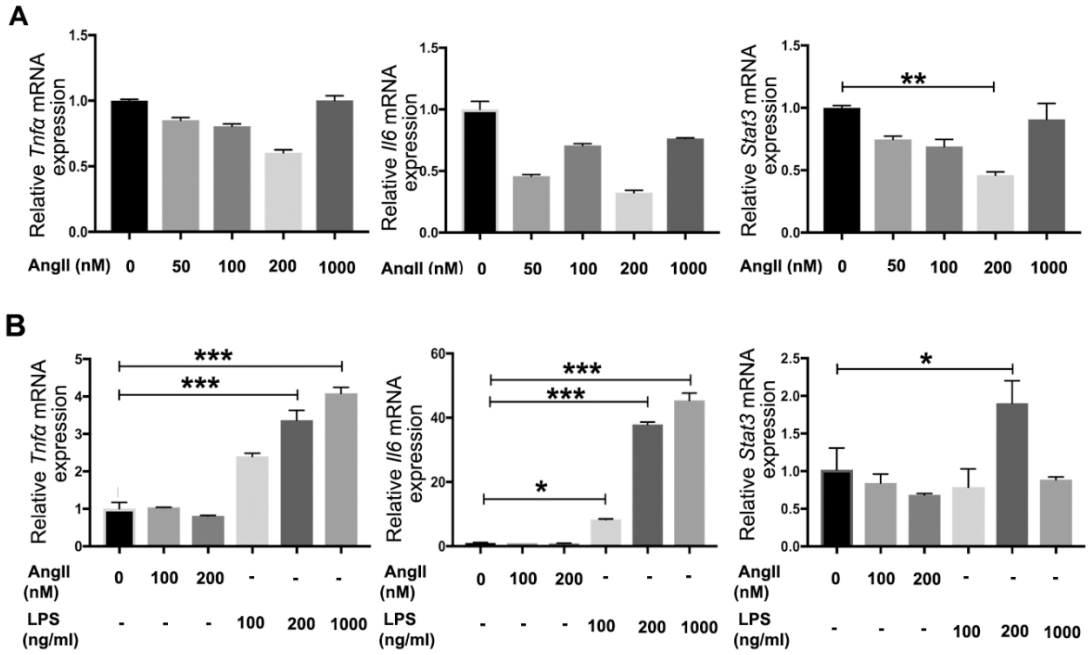

Appendix Figure 8. Different concentration of Ang II and LPS stimulation in raw264.7. Relative expression levels of *Tnfα, Il6* and *Stat3* in raw264.7 were detected by qRT-PCR at 24 hours after initial AngII or LPS stimulation. *Gapdh* was used as the endogenous control. *: p<0.05, **: p<0.01, ***: p<0.001, repeated 3 times.

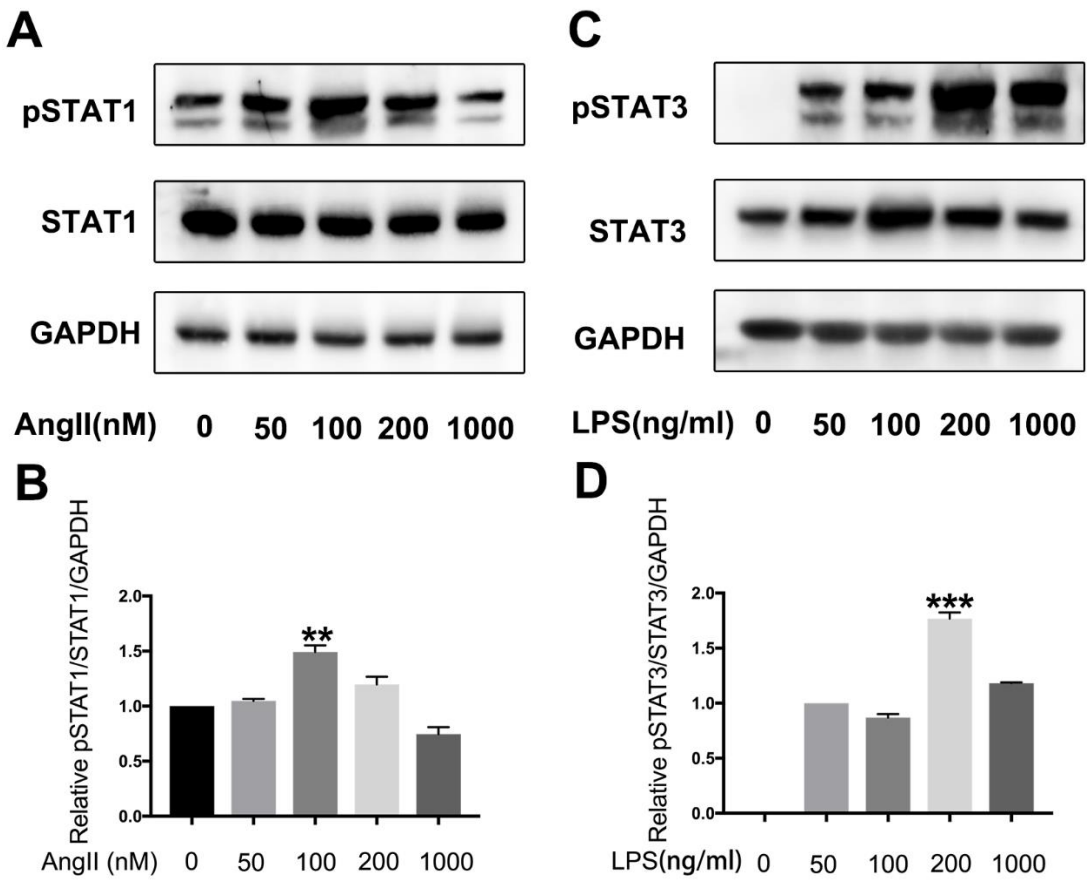

Appendix Figure 9. STATs proteins expression with different concentration of Ang II or LPS stimulation. (A) Western blot analysis of pSTAT1, STAT1 expression in different concentration of Ang II groups, representative images are shown. **(B)** Quantification of the normalized pSTAT1/STAT1. **(C)** Western blot analysis of pSTAT3, STAT3 expression in different concentration of LPS groups, representative images are shown. **(D)** Quantification of the normalized pSTAT3/STAT3**.** **: $p<0.01$, ***: $p<0.001$, repeated 3 times. Data are presented as the mean ± SD (n = 10 per group), compared with the Control.

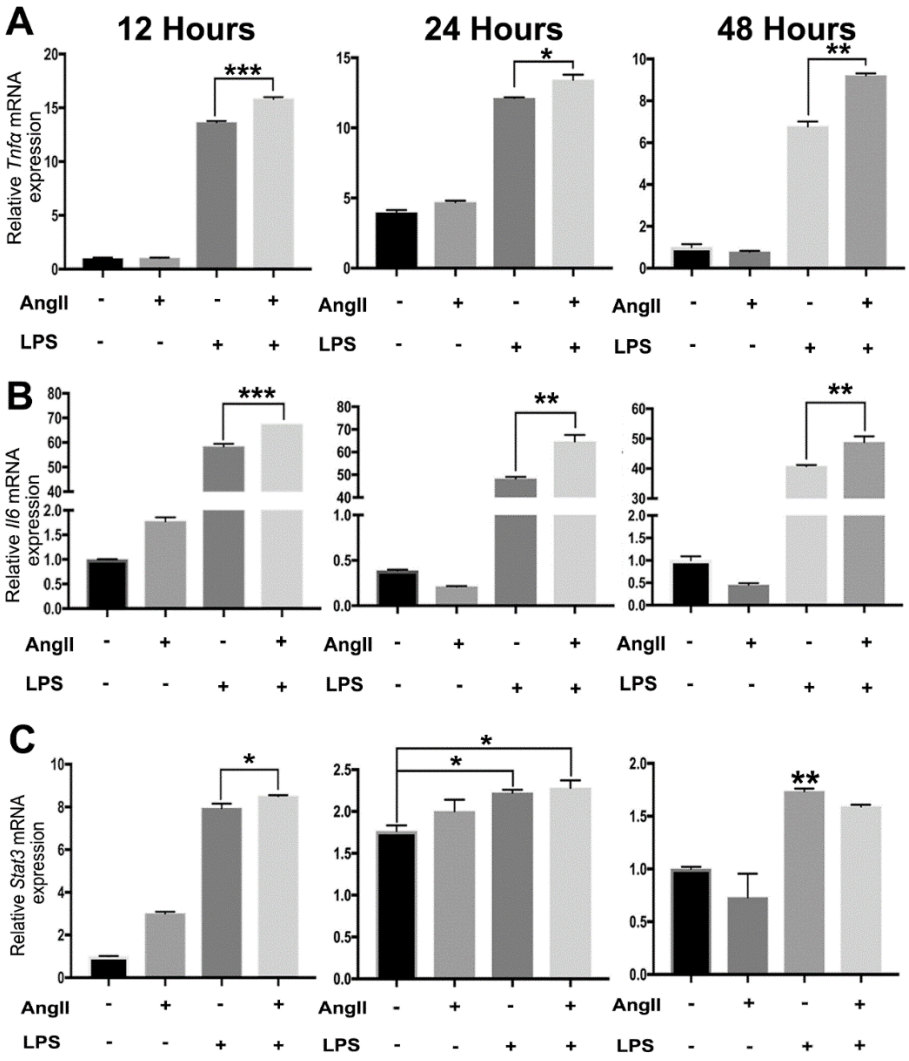

Appendix Figure 10. Different time period of Ang II and LPS stimulation in raw264.7. Relative expression levels of *Tnfα*，*Il6 and Stat3* in raw264.7 were detected by qRT-PCR at different time course after initial AngII or LPS stimulation. *Gapdh* was used as the endogenous control. *: p<0.05, **: p<0.01, ***: p<0.001, repeated 3 times. Data are presented as the mean ± SD (n = 10 per group), compared with the Control.

Appendix Table 1. Primers used in qRT-PCR.

Gene	FP (5' to 3')	RP (5' to 3')
Stat1	TCACAGTGGTTCGAGCTTCAG	GCAAACGAGACATCATAGGCA
Cxcl9	TCCTTTTGGGCATCATCTTCC	TTTGTAGTGGATCGTGCCTCG
Socs3	ATGGTCACCCACAGCAAGTTT	TCCAGTAGAATCCGCTCTCCT
Il6	CTCTGCAAGAGACTTCCATCCAGT	GAAGTAGGGAAGGCCGTGG
Tnfα	AGGGTCTGGGCCATAGAACT	CCACCACGCTCTTCTGTCTAC
Il1β	CAACCAACAAGTGATATTCTCCATG	ATCCACACTCTCCAGCTGCA
Ifnγ	AAACAATTTCTCCAGCACTG	ATTCTGAGGCATCAACTGAC
Stat3	CAATACCATTGACCTGCCGAT	GAGCGACTCAAACTGCCCT
Il10	AGCCTTATCGGAAATGATCCAGT	GGCCTTGTAGACACCTTGGT
F4/80	TGACTCACCTTGTGGTCCTAA	CTTCCCAGAATCCAGTCTTTCC
CD3	ATGCGGTGGAACACTTTCTGG	GCACGTCAACTCTACACTGGT
CD11b	ATGGACGCTGATGGCAATACC	TCCCCATTCACGTCTCCCA
CD19	GGAGGCAATGTTGTGCTGC	ACAATCACTAGCAAGATGCCC
AngII	TCTCCTTTACCACAACAAGAGCA	CTTCTCATTCACAGGGGAGGT
Nos3	GGCTGGGTTTAGGGCTGTG	CTGAGGGTGTCGTAGGTGATG
Agtrap	ATGCTTGGGGCAACTTCACTA	GCAGCAAGAGAAGGGCTTCA
Tlr4	ATGGCATGGCTTACACCACC	GAGGCCAATTTTGTCTCCACA
Gapdh	AGGTTGTCTCCTGCGACTTCA	CCAGGAAATGAGCTTGACAAA

References

Beklen A, Hukkanen M, Richardson R, Konttinen YT. 2008. Immunohistochemical localization of toll-like receptors 1-10 in periodontitis. Oral Microbiol Immunol. 23(5):425-431.

Daugherty A, Rateri D, Hong L, Balakrishnan A. 2009. Measuring blood pressure in mice using volume pressure recording, a tail-cuff method. J Vis Exp. (27).

Francke A, Herold J, Weinert S, Strasser RH, Braun-Dullaeus RC. 2011. Generation of mature murine monocytes from heterogeneous bone marrow and description of their properties. J Histochem Cytochem. 59(9):813-825.

Li J, Xiao X, Wei W, Ding H, Yue Y, Tian Y, Nabar N, Liu Z, Yang Z, Wang M. 2019. Inhibition of angiotensin ii receptor i prevents inflammation and bone loss in periodontitis. J Periodontol. 90(2):208-216.

Meng F, Lowell C. 1997. Lipopolysaccharide (lps)-induced macrophage activation and signal transduction in the absence of src-family kinases hck, fgr, and lyn. J Exp Med. 185(9):1661-1670.

Meng Y, Chen C, Liu Y, Tian C, Li H. 2017. Angiotensin ii regulates dendritic cells through activation of nf-kappab /p65, erk1/2 and stat1 pathways. Cell Physiol Biochem. 42(4):1550-1558.

Nogueira AV, de Souza JA, de Molon RS, Pereira Eda S, de Aquino SG, Giannobile WV, Cirelli JA. 2014. Hmgb1 localization during experimental periodontitis. Mediators Inflamm. 2014:816320.

Park CH, Abramson ZR, Taba M, Jr., Jin Q, Chang J, Kreider JM, Goldstein SA, Giannobile WV. 2007. Three-dimensional micro-computed tomographic imaging of alveolar bone in experimental bone loss or repair. J Periodontol. 78(2):273-281.

Sasaki H, Suzuki N, Kent R, Jr., Kawashima N, Takeda J, Stashenko P. 2008. T cell response mediated by myeloid cell-derived il-12 is responsible for porphyromonas gingivalis-induced periodontitis in il-10-deficient mice. J Immunol. 180(9):6193-6198.